

The Bosonic Quantum Breakdown Hubbard Model

Yu-Min Hu^{1,2} and Biao Lian²

¹*Institute for Advanced Study, Tsinghua University, Beijing, 100084, China*

²*Department of Physics, Princeton University, Princeton, NJ 08544, USA*

(Dated: January 10, 2024)

We propose a bosonic quantum breakdown Hubbard model, which generalizes the Bose-Hubbard model by adding an asymmetric breakdown interaction turning one boson into two between adjacent sites. We show that the ground state undergoes a first-order phase transition from Mott insulator to breakdown condensate as the breakdown interaction increases. When the normal hopping is zero, this model has a global exponential U(1) symmetry, which is spontaneously broken by the breakdown condensate, while the Mott-condensate transition remains first order. Surprisingly, the breakdown condensate with spontaneously broken exponential U(1) symmetry does not have a gapless Goldstone mode, which invalidates the Mermin-Wagner theorem and leads to stable spontaneous symmetry breaking in 1D. Moreover, we show that the model at non-equilibrium exhibits a dynamical transition from dielectric phase to breakdown phase with respect to the breakdown interaction. Our results show that quantum systems with exponential symmetry can exhibit novel unexpected properties.

Symmetries are central to the classification of quantum phases of matter. In particular, ground states with spontaneous broken global continuous symmetry are known to host gapless Goldstone modes. A prototypical example is the Bose-Hubbard model [1] for interacting bosons in a lattice, which exhibits a superfluid phase with spontaneously broken global U(1) symmetry and a linear dispersion Goldstone mode. In dimensions $d \leq 2$ ($d \leq 1$) at finite (zero) temperature, broken symmetries are generically restored by quantum fluctuations of the gapless Goldstone modes, according to the Mermin-Wagner theorem [2, 3].

In recent years, the study of phases of matter has been extended to various unconventional symmetries. For instance, dipole and multiple symmetries play a vital role in fractonic phases [4, 5], and the spontaneous breaking of dipole and multiple symmetries gives rise to exceptional quantum phases of matter [6–13]. Moreover, many of these unconventional symmetries exert substantial constraints on the non-equilibrium many-body quantum dynamics, such as Hilbert space fragmentation [14–19] and exotic relaxation hydrodynamics [20–26].

Recently, a distinct form of unconventional symmetry, known as exponential symmetry, has garnered attention in various contexts. The exponential U(1) symmetry is generated by an exponential charge $\hat{Q} = \sum_m q^{-m} \hat{n}_m$ with a certain number $q \neq 1$ and \hat{n}_m being the particle number at the m -th site. This symmetry has been found to play a significant role in exotic ground states [27, 28], topological phases [29–31], and constrained quantum dynamics [32–34]. In particular, in the quantum breakdown model for fermions [32], the exponential U(1) symmetry naturally arises from a spatially asymmetric *breakdown interaction* resembling the electrical breakdown phenomenon, leading to many-body localization.

This motivates us to propose a 1D bosonic quantum breakdown Hubbard model given in Eq. (1). It generalizes the celebrated Bose-Hubbard model [1] by adding

a spatially asymmetric breakdown interaction J which turns one boson in a site into two bosons in the next site (and vice versa). The model has a global exponential U(1) symmetry when the hopping $\gamma = 0$.

We study both the ground state phase diagram and the non-equilibrium quantum dynamics of this model. We find that the ground state generically exhibits a first-order phase transition from Mott insulator to breakdown condensate as the breakdown interaction J grows. Remarkably, at zero hopping, the phase transition remains first order, while the breakdown condensate spontaneously breaks the exponential U(1) symmetry. Most importantly, we find that the spontaneously broken global exponential U(1) symmetry does not give rise to gapless Goldstone modes, except for a single zero mode exactly corresponding to the exponential U(1) transformation. This invalidates the Mermin-Wagner theorem [2, 3], indicating that the spontaneous breaking of exponential U(1) symmetry is stable in any dimension $d > 0$. We also reveal a dynamical transition from a dielectric phase to a breakdown phase in the non-equilibrium quantum dynamics of the model as J increases, similar to [32]. Our results reveal unexpected novel properties of quantum matter with exponential symmetry.

Model. Inspired by the quantum breakdown model for fermions [32], we propose the *bosonic quantum breakdown Hubbard model* in a one-dimensional (1D) lattice of L sites. Each site m has a boson mode with annihilation and creation operators $\hat{a}_m, \hat{a}_m^\dagger$. The Hamiltonian is:

$$H = - \sum_{m=1}^{L-1} \left[\gamma \hat{a}_{m+1}^\dagger \hat{a}_m + J (\hat{a}_{m+1}^\dagger)^2 \hat{a}_m + \text{h.c.} \right] + \sum_{m=1}^L \left[-\mu \hat{n}_m + \frac{U}{2} \hat{n}_m (\hat{n}_m - 1) \right], \quad (1)$$

where $\hat{n}_m = \hat{a}_m^\dagger \hat{a}_m$ is the boson number on site m , and h.c. represents Hermitian conjugate. $\gamma \geq 0$ (real) is the

nearest neighbor hopping, μ is the chemical potential, and $U > 0$ is the on-site Hubbard interaction. Additionally, there is a spatially asymmetric interaction $J \geq 0$ (real) called the breakdown interaction [32], which induces a progressive proliferation (reduction) of bosons to the right (left) direction. This resembles the Townsend avalanche of numbers of particles (electrons and ions) in the electrical breakdown of dielectric gases. In ultracold atoms, such breakdown interaction for bosons has been studied in two-site systems, to elucidate the many-body chemical reactions of formation of diatomic molecules from atomic condensation [35–40]. In our model Eq. (1), the Hubbard interaction $U > 0$ ensures the total energy is lower bounded.

Exponential symmetry. When $\gamma > 0$ and $J > 0$, the model has no symmetry other than translation symmetry. However, additional global symmetry exists in the two cases below.

At $J = 0$ and $\gamma > 0$, the model in Eq. (1) reduces to the celebrated Bose-Hubbard model [1], which has a global U(1) symmetry $\hat{a}_m \rightarrow e^{i\varphi} \hat{a}_m$ corresponding to the conserved boson number $\hat{N}_{\text{tot}} = \sum_m \hat{n}_m$.

At $J > 0$ and $\gamma = 0$, the model has a symmetry dependent on the boundary condition. For the open boundary condition (OBC) that we assumed in Eq. (1), the model also has a global exponential U(1) symmetry given by

$$\hat{a}_m \rightarrow e^{i\varphi_m} \hat{a}_m, \quad \varphi_m = 2^{L-m} \varphi_L \quad (1 \leq m \leq L), \quad (2)$$

with $\varphi_L \in [0, 2\pi)$, and the associated conserved U(1) charge is $\hat{Q}^{(\text{OBC})} = \sum_{m=1}^L 2^{L-m} \hat{n}_m$. If one instead imposes periodic boundary condition (PBC), Eq. (2) would still be a symmetry if $\varphi_L = 2\varphi_1 \bmod 2\pi$, which requires $\varphi_L = \frac{2\pi p}{2^L - 1}$, $p \in \mathbb{Z}$. Thus, the model has a global $\mathbb{Z}_{2^L - 1}$ symmetry, and accordingly the conserved charge is $\hat{Q}^{(\text{PBC})} = \hat{Q}^{(\text{OBC})} \bmod (2^L - 1)$. This is similar to other PBC models with exponential symmetry studied recently [28–30]. In the limit $L \rightarrow \infty$, both OBC and PBC effectively have a U(1) symmetry. Note that this U(1) charge does not commute with translation, although the Hamiltonian is translationally invariant.

Ground-state phase diagram. We now investigate the ground state of our model Eq. (1). Our starting point is $\gamma = J = 0$, where the system comprises decoupled sites, and the ground state is a Mott insulator (MI) with an integer number of bosons $\langle \hat{n}_m \rangle = n \in \mathbb{Z}$ per site when $n - 1 \leq \mu/U \leq n$.

When $J = 0$, which reduces to the Bose-Hubbard model [1], for fixed $\mu > 0$, the mean-field ground state is known to undergo a U(1) spontaneous symmetry breaking (SSB) phase transition from MI to a boson condensate superfluid as γ/U increases, characterized by the continuous transition of the order parameter $\phi_m = \langle \hat{a}_m \rangle$ from zero to nonzero. The superfluid phase exhibits a gapless Goldstone mode with linear dispersion. By the Mermin-Wagner theorem [2, 3], the SSB of superfluid

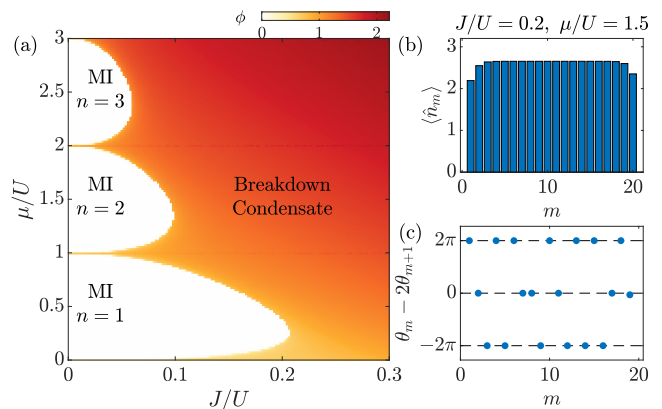


FIG. 1. (a) The ground state phase diagram of the model in Eq. (1) at $\gamma = 0$, and we set $U = 1$. The colormap shows the order parameter ϕ . (b) The ground state density $\langle \hat{n}_m \rangle$ and (c) a possible phase angle configuration $\theta_m = \arg[\phi_m]$ in the breakdown condensate ($J/U = 0.2$ and $\mu/U = 1.5$). The Gutzwiller mean-field ground state is calculated with $N_{\text{max}} = 20$ and $L = 20$.

becomes only quasi-long range ordered at zero temperature in 1D, due to quantum fluctuations of the Goldstone modes.

To extend the mean field theory to generic t and J , we employ a spatially dependent Gutzwiller mean-field ansatz wavefunction [41, 42]:

$$|\Phi\rangle = \prod_{m=1}^L \left(\sum_{n=0}^{N_{\text{max}}} C_{m,n} \frac{(\hat{a}_m^\dagger)^n}{\sqrt{n!}} \right) |0\rangle, \quad (3)$$

where $|0\rangle$ is the vacuum state, and we truncate the allowed boson number per site at some large enough N_{max} . We numerically minimize the energy density (for OBC) $\mathcal{E}_\Phi(\{C_{m,n}\}) = \frac{\langle \Phi | H | \Phi \rangle}{L \langle \Phi | \Phi \rangle}$ with respect to the complex variational parameters $C_{m,n}$, and find the mean field ground state $|\Phi_{\text{gs}}\rangle$ [43]. We then define the local complex order parameter ϕ_m and its mean magnitude ϕ as

$$\phi_m = \frac{\langle \Phi_{\text{gs}} | \hat{a}_m | \Phi_{\text{gs}} \rangle}{\langle \Phi_{\text{gs}} | \Phi_{\text{gs}} \rangle} = |\phi_m| e^{i\theta_m}, \quad \phi = \frac{1}{L} \sum_{m=1}^L |\phi_m|. \quad (4)$$

We also calculate the boson filling per site $\langle \hat{n}_m \rangle = \frac{\langle \Phi_{\text{gs}} | \hat{n}_m | \Phi_{\text{gs}} \rangle}{\langle \Phi_{\text{gs}} | \Phi_{\text{gs}} \rangle}$. At $J = 0$, this reproduces the phase diagram of the Bose-Hubbard model [1] with respect to μ/U and t/U .

In the $\gamma = 0$ case, which has the exponential U(1) symmetry in Eq. (2), the ground state phase diagram with respect to μ/U and J/U is shown in Fig. 1. We find the order parameter magnitude $|\phi_m|$ and the filling $\langle \hat{n}_m \rangle$ are always spatially uniform in the bulk [Fig. 1(b)]. At small J/U , there are isolated domes of MI phases with $\phi = 0$ and integer fillings $\langle \hat{n}_m \rangle = n \in \mathbb{Z}$. The large J/U space outside the MI phases is in a phase with order parameter $\phi > 0$ and thus U(1) SSB, which we

call the *breakdown condensate* phase. The phase angles $\theta_m = \arg(\phi_m)$ in Eq. (4) are locked to satisfy $\theta_m = 2\theta_{m+1} \bmod 2\pi$ as shown in Fig. 1(c). Therefore, by U(1) phase rotation in Eq. (2), one can rotate the order parameter into $\theta_m = 0$, after which $\phi_m = \phi > 0$ is real positive and uniform.

Unexpectedly, we find the phase boundary in Fig. 1(a) between MI and the SSB breakdown condensate in the $\gamma = 0$ case is everywhere of the first order. This can be seen in Fig. 2(c), where ϕ jumps discontinuously from zero to nonzero at the phase boundary. This is due to the competition between different energy minima existing in the ϕ space. This is in sharp contrast with the $J = 0$ Bose-Hubbard model case, in which ϕ is known to undergo a continuous second-order phase transition at the phase boundary [Fig. 2(b)].

In the generic case $\gamma > 0$ and $J > 0$, the absence of global symmetry other than translation forces the phase boundaries between translationally invariant phases to be of the first order. Indeed, for fixed μ , we find two phases: MI and breakdown condensate, which are separated by a first-order phase boundary for $\gamma > 0$ and $J > 0$, as shown in Fig. 2(a). The bulk of breakdown condensate has $\phi_m = \phi$ being real and positive. The only second-order phase transition point is the Bose-Hubbard model phase transition on the γ/U axis at $J = 0$ [Fig. 2(b)], for which the breakdown condensate reduces to the superfluid phase.

Excitations. To examine the low-energy excitations in the breakdown condensate, we consider the order parameter of the form $\phi_m = \sqrt{\bar{\rho} + \delta\rho_m} e^{i\delta\theta_m}$, with phase fluctuations $\delta\theta_m$ and density fluctuations $\delta\rho_m$. The Lagrangian for model Eq. (1) with OBC reads $\mathcal{L} = \frac{1}{2} \sum_{m=1}^L (i\phi_m^* \partial_t \phi_m - i\phi_m \partial_t \phi_m^*) - \langle H \rangle = \mathcal{L}_0 + \delta\mathcal{L}$, where \mathcal{L}_0 is the Lagrangian of the mean field ground state with constant particle density $\bar{\rho} = \phi^2 > 0$. Deep in the breakdown condensate phase, which is well described by a coherent state obeying $\hat{a}_m|\Phi\rangle = \phi_m|\Phi\rangle$, $\bar{\rho}$ satisfies the saddle-point equation $\mu + 2\gamma + 3J\sqrt{\bar{\rho}} - U\bar{\rho} = 0$, and the Lagrangian fluctuation $\delta\mathcal{L}$ expanded to the second order (up to total derivatives) reads

$$\begin{aligned} \delta\mathcal{L} \approx & - \sum_{m=1}^L \left[\delta\rho_m \partial_t \delta\theta_m + \frac{U}{2} \delta\rho_m^2 \right] \\ & - \sum_{m=1}^{L-1} \left[J\bar{\rho}^{\frac{3}{2}} (\delta\theta_m - 2\delta\theta_{m+1})^2 + \gamma\bar{\rho} (\delta\theta_m - \delta\theta_{m+1})^2 \right] \\ & + \frac{J}{4\sqrt{\bar{\rho}}} (\delta\rho_m^2 - 4\delta\rho_m \delta\rho_{m+1}) + \frac{\gamma}{4\bar{\rho}} (\delta\rho_m - \delta\rho_{m+1})^2 \Big] \\ = & -\delta\boldsymbol{\rho}^T \partial_t \delta\boldsymbol{\theta} - \delta\boldsymbol{\theta}^T M_\theta \delta\boldsymbol{\theta} - \frac{1}{4} \delta\boldsymbol{\rho}^T M_\rho \delta\boldsymbol{\rho} , \end{aligned} \quad (5)$$

where we have defined $\delta\boldsymbol{\theta} \equiv (\delta\theta_1, \dots, \delta\theta_L)^T$ and $\delta\boldsymbol{\rho} \equiv (\delta\rho_1, \dots, \delta\rho_L)^T$, while the coefficients are rewritten into matrices M_θ which is non-negative and M_ρ which is positive definite [43]. Integrating out $\delta\rho_m$ yields an effective

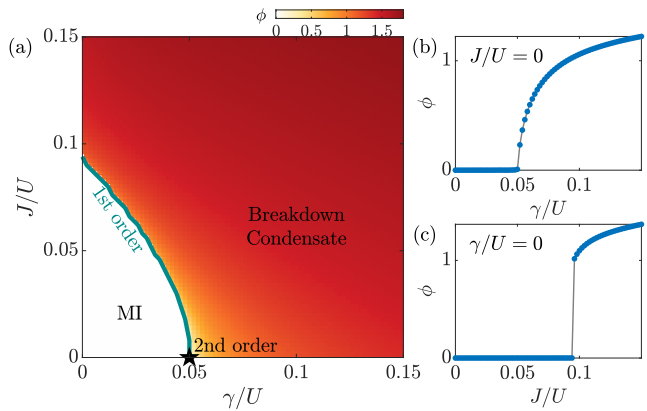


FIG. 2. (a) The ground state phase diagram at fixed $U = 1$ and $\mu/U = 1.5$. (b) The order parameter ϕ at $J = 0$ versus γ/U (reduced to the Bose-Hubbard model). (c) The order parameter ϕ at $\gamma = 0$ versus J/U . The calculation is done with $N_{\max} = 20$ and $L = 20$.

Lagrangian $\delta\mathcal{L}_{\text{eff}} = \partial_t \delta\boldsymbol{\theta}^T M_\rho^{-1} \partial_t \delta\boldsymbol{\theta} - \delta\boldsymbol{\theta}^T M_\theta \delta\boldsymbol{\theta}$. Consequently, the Euler-Lagrange equation reads

$$\partial_t^2 \delta\boldsymbol{\theta}(t) = -D \delta\boldsymbol{\theta}(t) , \quad D = M_\rho M_\theta . \quad (6)$$

The excitation energies ω are square roots of the eigenvalues of the above dynamical matrix D .

Fig. 3 shows the excitation spectrum for $L = 50$ with OBC at different J and γ . At $J = 0$ and $\gamma > 0$, we obtain a linear dispersion gapless Goldstone mode as expected in the conventional superfluid. At $J > 0$ and $\gamma \geq 0$, we generically find a fully gapped bulk spectrum with $\delta\theta_m$ eigenmodes extended in the bulk [blue thin lines in Fig. 3(a)-(d)], and a single in-gap low-lying edge mode with $\delta\theta_m$ exponentially localized at the left edge [red bold lines in Fig. 3(a)-(d)].

Specifically, when $J > 0$ and $\gamma = 0$, in which case the model has the exponential U(1) symmetry in Eq. (2) spontaneously broken by the breakdown condensate, the single edge mode of the breakdown condensate reaches zero energy, while the bulk spectrum remains gapped. The edge mode is given by $\delta\theta_m = 2^{-m} \delta\theta_0$, which is exactly the exponential U(1) phase rotation, thus has zero energy. Therefore, there is no gapless Goldstone mode other than the symmetry transformation. Importantly, the absence of gapless excitations invalidates the Mermin-Wagner theorem, and thus we expect the spontaneous exponential U(1) symmetry breaking of the breakdown condensate to survive up to a finite critical temperature T_c .

The absence of gapless Goldstone mode originates from non-commutation of the exponential U(1) charge with translation, which can be seen as follows. By a similarity transformation $\delta\theta_m = 2^{-m} \alpha_m$, the exponential U(1) transformation Eq. (2) becomes homogeneously $\alpha_m \rightarrow \alpha_m + \varphi_0$. Taking the continuum limit $\alpha_m(t) \rightarrow \alpha(x, t)$, we find the effective Lagrangian at $\gamma = 0$ has the inho-

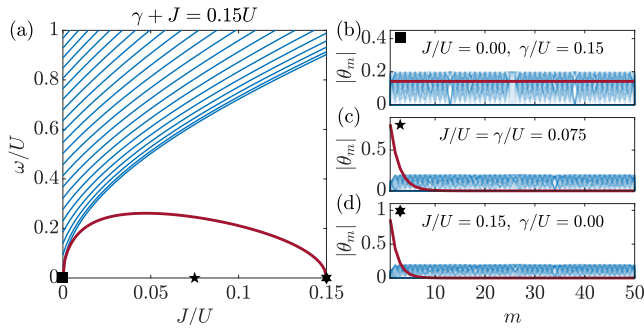


FIG. 3. (a) The excitation energy spectra of Eq. (6) in the breakdown condensate with OBC. The parameters are fixed at $U = 1$, $J + \gamma = 0.15U$ and $\mu/U = 1.5$. (b-d) Eigen-wavefunctions of the dynamical matrix D for parameters marked as points in (a). In all panels, bulk states are denoted by blue lines, while the red line denotes the lowest eigenstate which is the only edge mode when $J > 0$.

homogeneous form $\delta\mathcal{L}_{\text{eff}} \approx g(x) [(\partial_t\alpha)^2 - v^2(\partial_x\alpha)^2]$, where $g(x) \approx g(0)e^{-2x/\xi}$ with $\xi = \frac{1}{\ln 2}$ and $v > 0$. This resembles a massless Klein-Gordon field in a curved spacetime, which yields an Euler-Lagrange equation

$$(v^{-2}\partial_t^2 - \partial_x^2 + 2\xi^{-1}\partial_x)\alpha = 0. \quad (7)$$

This corresponds to the celebrated Hatano-Nelson model [44, 45], a non-Hermitian dynamical matrix that has a gapped real energy spectrum $\omega = v\sqrt{\xi^{-2} + k^2}$ (with k real) under OBC, with eigenmodes $\alpha(x, t) = \alpha_0 e^{(\xi^{-1} + ik)x - i\omega t}$ exhibiting the non-Hermitian skin effect [46]. Note that such eigenmodes are bulk plane waves $\delta\theta(x, t) = \delta\theta_0 e^{ikx - i\omega t}$ when transformed back to the $\delta\theta_m$ basis. The zero energy mode $\alpha(x, t) = \alpha_0$ corresponds to the edge mode in the $\delta\theta_m$ basis.

Quantum dynamics. In the fermionic quantum breakdown model in Ref. [32], a dynamical transition resembling the electrical breakdown is revealed. We now investigate such breakdown transition in the dynamical evolution of the bosonic model in Eq. (1). We restrict ourselves to the $\gamma = 0$ case with OBC, for which we can do exact diagonalization (ED) in a certain charge sector of the exponential U(1) charge \hat{Q}^{OBC} , which is finite dimensional for finite lattice size L .

We specifically focus on the quench dynamics of the state $|\Psi_0\rangle = \hat{a}_1^\dagger|0\rangle$ with only a single boson at the first site, which is in the $\hat{Q}^{\text{OBC}} = 2^{L-1}$ charge sector. In our ED we take $L = 7$, and this charge sector has a Hilbert space dimension $d_Q = 1828$. We set $\mu < 0$, such that the ground state in the $J/U \rightarrow 0$ limit is the particle vacuum $|0\rangle$, resembling the dielectrics before electrical breakdown. We calculate the evolution of the boson number $\langle \hat{n}_m(t) \rangle = \langle \Psi_0 | e^{iHt} \hat{n}_m e^{-iHt} | \Psi_0 \rangle$ at each site with respect to time t , and define the long-time average of the boson number as $\bar{n}_m = \lim_{T \rightarrow \infty} \frac{1}{T} \int_0^T dt \langle \hat{n}_m(t) \rangle$. If the breakdown happens, one expects the boson on site 1 to

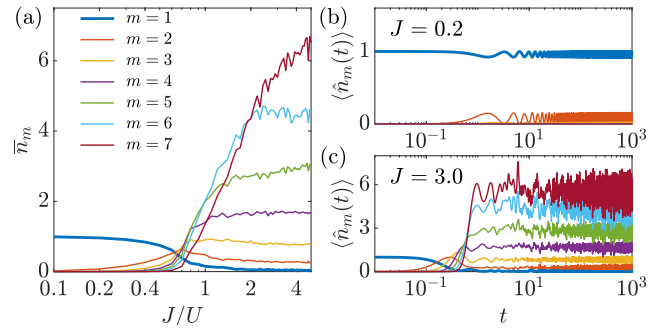


FIG. 4. (a) The dynamical breakdown transition as J increases, where we set $\mu = -1$, $U = 1$, $\gamma = 0$, and $L = 7$, with the initial state $|\Psi_0\rangle = \hat{a}_1^\dagger|0\rangle$. The colored lines are the time-averaged (over time $T = 10^3$) boson numbers \bar{n}_m on site m . (b) and (c) The time evolution of the boson numbers $\langle \hat{n}_m(t) \rangle$ when $J = 0.2$ and $J = 3.0$ respectively.

evolve into many bosons on later sites.

Fig. 4(a) shows \bar{n}_m calculated over time $T = 10^3$, where we fix $\mu = -1$, $U = 1$. A clear breakdown transition at $J/U \approx 0.7$ can be observed. When $J/U < 0.7$, the system is in the dielectric phase with the boson bounded at the site $m = 1$. When $J/U > 0.7$, the system enters the breakdown phase where the $m > 1$ sites are filled with many bosons. Fig. 4(b) and (c) show the time evolution of $\langle \hat{n}_m(t) \rangle$ in the dielectric and breakdown phases, respectively.

The breakdown transition can be understood as follows. Via the hopping from one boson on site 1 to two bosons on site 2, the system approximately gains an energy $2|\langle 0 | \frac{(\hat{a}_2)^2}{\sqrt{2}} H \hat{a}_1^\dagger | 0 \rangle| = 2\sqrt{2}J$. However, the two-boson state costs an on-site energy $U - \mu$ more than the one-boson state. Thus, the breakdown happens only if the energy gain is larger:

$$2\sqrt{2}J > U - \mu, \quad (8)$$

which approximately agrees with the breakdown transition observed in Fig. 4(a).

Furthermore, we find the level spacing statistics of the charge sector shows a crossover from Poisson to Wigner-Dyson as J/U increases [43]. We thus expect the model to be quantum chaotic in the breakdown phase, quickly approaching thermal equilibrium. This agrees with Fig. 4(c) in the breakdown phase, where the boson on site 1 decays in a time scale $\sim J^{-1}$, after which the system is approximately in equilibrium.

Discussions. We have shown that the ground state of 1D bosonic quantum breakdown Hubbard model exhibits Mott insulator phases and a breakdown condensate phase, separated by a first-order phase boundary. Most strikingly, at zero hopping ($\gamma = 0$), the breakdown condensate spontaneously breaks the global exponential U(1) symmetry in Eq. (2), but has no gapless Goldstone mode, which effectively maps to a non-Hermitian dynamical

ical matrix of massless bosons in curved spacetime[47]. This invalidates the Mermin-Wagner theorem and stabilizes the condensate in 1D. We expect similar conclusions to hold in higher dimensional generalizations of our model. An intriguing future question is to investigate generic conditions for spontaneous global symmetry breaking without gapless Goldstone modes. We also reveal a breakdown transition in the quench dynamics of our model. This property may be utilized as a particle detector in theoretical studies. It will also be greatly interesting to explore the realization of such models in experimental platforms such as ultracold atoms [35, 36].

Acknowledgements. We thank Bo-Ting Chen, Hao Chen, Yichen Hu, Zhou-Quan Wan, Shunyu Yao, and Wucheng Zhang for helpful discussions. Y.-M. Hu acknowledges the support from NSFC under Grant No. 12125405 and the Tsinghua Visiting Doctoral Students Foundation. This work is supported by the Alfred P. Sloan Foundation, the National Science Foundation through Princeton University’s Materials Research Science and Engineering Center DMR-2011750, and the National Science Foundation under award DMR-2141966. Additional support is provided by the Gordon and Betty Moore Foundation through Grant GBMF8685 towards the Princeton theory program.

-
- [1] M. P. A. Fisher, P. B. Weichman, G. Grinstein, and D. S. Fisher, Boson localization and the superfluid-insulator transition, *Phys. Rev. B* **40**, 546 (1989).
- [2] N. D. Mermin and H. Wagner, Absence of ferromagnetism or antiferromagnetism in one- or two-dimensional isotropic heisenberg models, *Phys. Rev. Lett.* **17**, 1133 (1966).
- [3] P. C. Hohenberg, Existence of long-range order in one and two dimensions, *Phys. Rev.* **158**, 383 (1967).
- [4] R. M. Nandkishore and M. Hermele, Fractons, *Annual Review of Condensed Matter Physics* **10**, 295 (2019).
- [5] M. Pretko, X. Chen, and Y. You, Fracton phases of matter, *International Journal of Modern Physics A* **35**, 2030003 (2020).
- [6] J.-K. Yuan, S. A. Chen, and P. Ye, Fractonic superfluids, *Phys. Rev. Res.* **2**, 023267 (2020).
- [7] S. A. Chen, J.-K. Yuan, and P. Ye, Fractonic superfluids. ii. condensing subdimensional particles, *Phys. Rev. Res.* **3**, 013226 (2021).
- [8] A. Kapustin and L. Spodyneiko, Hohenberg-mermin-wagner-type theorems and dipole symmetry, *Phys. Rev. B* **106**, 245125 (2022).
- [9] C. Stahl, E. Lake, and R. Nandkishore, Spontaneous breaking of multipole symmetries, *Phys. Rev. B* **105**, 155107 (2022).
- [10] E. Lake, M. Hermele, and T. Senthil, Dipolar bose-hubbard model, *Phys. Rev. B* **106**, 064511 (2022).
- [11] S. A. Chen and P. Ye, Many-body physics of spontaneously broken higher-rank symmetry: from fractonic superfluids to dipolar hubbard model (2023), [arXiv:2305.00941 \[cond-mat.str-el\]](https://arxiv.org/abs/2305.00941).
- [12] P. Zechmann, E. Altman, M. Knap, and J. Feldmeier, Fractonic luttinger liquids and supersolids in a constrained bose-hubbard model, *Phys. Rev. B* **107**, 195131 (2023).
- [13] J. Boesl, P. Zechmann, J. Feldmeier, and M. Knap, Deconfinement dynamics of fractons in tilted bose-hubbard chains (2023), [arXiv:2311.08455 \[cond-mat.quant-gas\]](https://arxiv.org/abs/2311.08455).
- [14] V. Khemani, M. Hermele, and R. Nandkishore, Localization from hilbert space shattering: From theory to physical realizations, *Phys. Rev. B* **101**, 174204 (2020).
- [15] P. Sala, T. Rakovszky, R. Verresen, M. Knap, and F. Pollmann, Ergodicity breaking arising from hilbert space fragmentation in dipole-conserving hamiltonians, *Phys. Rev. X* **10**, 011047 (2020).
- [16] S. Moudgalya, A. Prem, R. Nandkishore, N. Regnault, and B. A. Bernevig, Thermalization and its absence within krylov subspaces of a constrained hamiltonian, in *Memorial Volume for Shoucheng Zhang* (World Scientific, 2022) pp. 147–209.
- [17] S. Moudgalya and O. I. Motrunich, Hilbert space fragmentation and commutant algebras, *Phys. Rev. X* **12**, 011050 (2022).
- [18] S. Moudgalya, B. A. Bernevig, and N. Regnault, Quantum many-body scars and hilbert space fragmentation: a review of exact results, *Reports on Progress in Physics* **85**, 086501 (2022).
- [19] T. Kohlert, S. Scherg, P. Sala, F. Pollmann, B. Hebbe Madhusudhana, I. Bloch, and M. Aidelsburger, Exploring the regime of fragmentation in strongly tilted fermi-hubbard chains, *Phys. Rev. Lett.* **130**, 010201 (2023).
- [20] J. Feldmeier, P. Sala, G. De Tomasi, F. Pollmann, and M. Knap, Anomalous diffusion in dipole- and higher-moment-conserving systems, *Phys. Rev. Lett.* **125**, 245303 (2020).
- [21] P. Zhang, Subdiffusion in strongly tilted lattice systems, *Phys. Rev. Res.* **2**, 033129 (2020).
- [22] O. Ogunnaike, J. Feldmeier, and J. Y. Lee, Unifying emergent hydrodynamics and lindbladian low energy spectra across symmetries, constraints, and long-range interactions (2023), [arXiv:2304.13028 \[cond-mat.str-el\]](https://arxiv.org/abs/2304.13028).
- [23] A. Morningstar, N. O’Dea, and J. Richter, Hydrodynamics in long-range interacting systems with center-of-mass conservation, *Phys. Rev. B* **108**, L020304 (2023).
- [24] J. Gliozzi, J. May-Mann, T. L. Hughes, and G. De Tomasi, Hierarchical hydrodynamics in long-range multipole-conserving systems, *Phys. Rev. B* **108**, 195106 (2023).
- [25] C. Stahl, M. Qi, P. Glorioso, A. Lucas, and R. Nandkishore, Fracton superfluid hydrodynamics, *Phys. Rev. B* **108**, 144509 (2023).
- [26] A. Jain, K. Jensen, R. Liu, and E. Mefford, Dipole superfluid hydrodynamics (2023), [arXiv:2304.09852 \[hep-th\]](https://arxiv.org/abs/2304.09852).
- [27] P. Sala, Y. You, J. Hauschild, and O. Motrunich, Exotic quantum liquids in bose-hubbard models with spatially-modulated symmetries (2023), [arXiv:2307.08761 \[cond-mat.quant-gas\]](https://arxiv.org/abs/2307.08761).
- [28] Y. Hu and H. Watanabe, Spontaneous symmetry breaking without ground state degeneracy in generalized n -state clock model, *Phys. Rev. B* **107**, 195139 (2023).
- [29] H. Watanabe, M. Cheng, and Y. Fuji, Ground state degeneracy on torus in a family of ZN toric code, *Journal of Mathematical Physics* **64**, 051901 (2023).
- [30] G. Delfino, C. Chamon, and Y. You, 2d frac-

- tons from gauging exponential symmetries (2023), [arXiv:2306.17121 \[cond-mat.str-el\]](#).
- [31] J. H. Han, E. Lake, H. T. Lam, R. Verresen, and Y. You, Topological quantum chains protected by dipolar and other modulated symmetries (2023), [arXiv:2309.10036 \[cond-mat.str-el\]](#).
- [32] B. Lian, Quantum breakdown model: From many-body localization to chaos with scars, *Phys. Rev. B* **107**, 115171 (2023).
- [33] X. Liu and B. Lian, 2d quantum breakdown model with krylov subspace many-body localization (2023), [arXiv:2311.10968 \[cond-mat.str-el\]](#).
- [34] P. Sala, J. Lehmann, T. Rakovszky, and F. Pollmann, Dynamics in systems with modulated symmetries, *Phys. Rev. Lett.* **129**, 170601 (2022).
- [35] Z. Zhang, L. Chen, K.-X. Yao, and C. Chin, Transition from an atomic to a molecular bose-einstein condensate, *Nature* **592**, 708 (2021).
- [36] Z. Zhang, S. Nagata, K.-X. Yao, and C. Chin, Many-body chemical reactions in a quantum degenerate gas, *Nature Physics* **19**, 1466 (2023).
- [37] D. J. Heinzen, R. Wynar, P. D. Drummond, and K. V. Kheruntsyan, Superchemistry: Dynamics of coupled atomic and molecular bose-einstein condensates, *Phys. Rev. Lett.* **84**, 5029 (2000).
- [38] L. Radzihovsky, J. Park, and P. B. Weichman, Superfluid transitions in bosonic atom-molecule mixtures near a feshbach resonance, *Phys. Rev. Lett.* **92**, 160402 (2004).
- [39] M. W. J. Romans, R. A. Duine, S. Sachdev, and H. T. C. Stoof, Quantum phase transition in an atomic bose gas with a feshbach resonance, *Phys. Rev. Lett.* **93**, 020405 (2004).
- [40] R. K. Malla, V. Y. Chernyak, C. Sun, and N. A. Sinitsyn, Coherent reaction between molecular and atomic bose-einstein condensates: Integrable model, *Phys. Rev. Lett.* **129**, 033201 (2022).
- [41] W. Krauth, M. Caffarel, and J.-P. Bouchaud, Gutzwiller wave function for a model of strongly interacting bosons, *Phys. Rev. B* **45**, 3137 (1992).
- [42] K. V. Krutitsky and P. Navez, Excitation dynamics in a lattice bose gas within the time-dependent gutzwiller mean-field approach, *Phys. Rev. A* **84**, 033602 (2011).
- [43] See the supplemental materials, which include Ref. [48, 49].
- [44] N. Hatano and D. R. Nelson, Localization transitions in non-hermitian quantum mechanics, *Phys. Rev. Lett.* **77**, 570 (1996).
- [45] N. Hatano and D. R. Nelson, Vortex pinning and non-hermitian quantum mechanics, *Phys. Rev. B* **56**, 8651 (1997).
- [46] S. Yao and Z. Wang, Edge states and topological invariants of non-hermitian systems, *Phys. Rev. Lett.* **121**, 086803 (2018).
- [47] C. Lv, R. Zhang, Z. Zhai, and Q. Zhou, Curving the space by non-hermiticity, *Nature communications* **13**, 2184 (2022).
- [48] V. Oganesyan and D. A. Huse, Localization of interacting fermions at high temperature, *Phys. Rev. B* **75**, 155111 (2007).
- [49] Y. Y. Atas, E. Bogomolny, O. Giraud, and G. Roux, Distribution of the ratio of consecutive level spacings in random matrix ensembles, *Phys. Rev. Lett.* **110**, 084101 (2013).

THE SUPPLEMENTAL MATERIALS

Coefficient matrices in the effective Lagrangian

In the main text, we have derived an effective Lagrangian to describe the low-energy phase fluctuations of the breakdown condensate. This Lagrangian is given by

$$\delta\mathcal{L}_{\text{eff}} = \partial_t\delta\theta^T M_\rho^{-1}\partial_t\delta\theta - \delta\theta^T M_\theta\delta\theta. \quad (9)$$

In this section, we provide explicit formulations for the coefficient matrices M_ρ and M_θ of dimension $L \times L$, with L being the lattice length. These expressions are extracted directly from Eq. (5) in the main text. With \mathbb{I} being the identity matrix of dimension L , the expressions are given by

$$M_\rho = 2U\mathbb{I} + \frac{J}{\sqrt{\rho}} \begin{pmatrix} 1 & -2 & & & & \\ -2 & 1 & -2 & & & \\ & & \ddots & \ddots & \ddots & \\ & & & -2 & 1 & -2 \\ & & & & -2 & 0 \end{pmatrix} + \frac{\gamma}{\rho} \begin{pmatrix} 1 & -1 & & & & \\ -1 & 2 & -1 & & & \\ & & \ddots & \ddots & \ddots & \\ & & & -1 & 2 & -1 \\ & & & & -1 & 1 \end{pmatrix}, \quad (10)$$

$$M_\theta = J\rho^{\frac{3}{2}} \begin{pmatrix} 1 & -2 & & & & \\ -2 & 5 & -2 & & & \\ & & \ddots & \ddots & \ddots & \\ & & & -2 & 5 & -2 \\ & & & & -2 & 4 \end{pmatrix} + \gamma\rho \begin{pmatrix} 1 & -1 & & & & \\ -1 & 2 & -1 & & & \\ & & \ddots & \ddots & \ddots & \\ & & & -1 & 2 & -1 \\ & & & & -1 & 1 \end{pmatrix}.$$

The level spacing statistics of the $\hat{Q}^{\text{OBC}} = 2^{L-1}$ charge sector

In this section, we employ exact diagonalization techniques to study the level spacing statistics of the $\gamma = 0$

bosonic quantum breakdown Hubbard model. Specifically, we focus on the charge sector $\hat{Q}^{\text{OBC}} = 2^{L-1}$. This

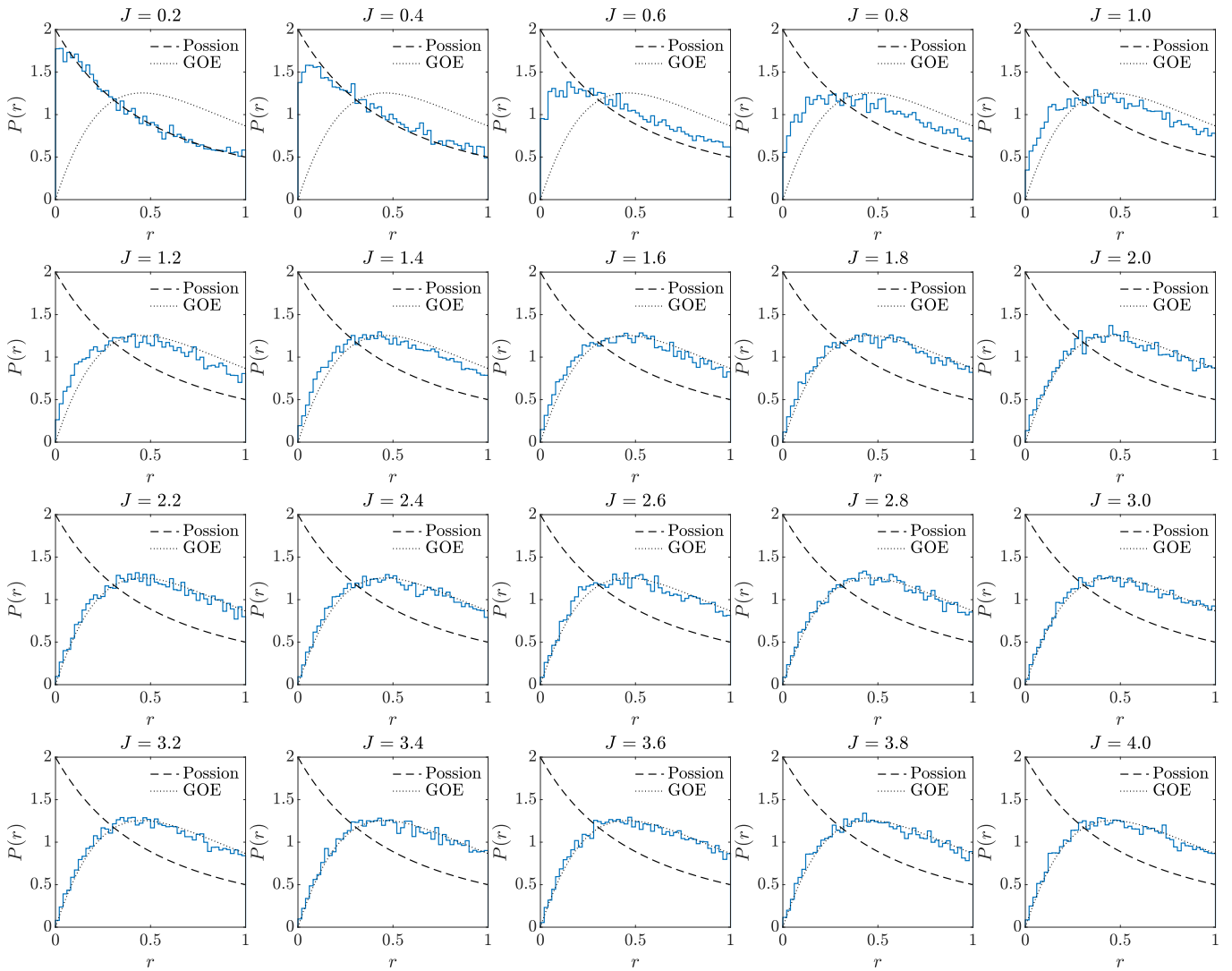


FIG. 5. The distribution $P(r)$ of r_n for varying values of J/U in the $\hat{Q}^{\text{OBC}} = 2^{L-1}$ charge sector, with fixed parameters set as $U = 1$, $\mu = -1$, and $L = 8$.

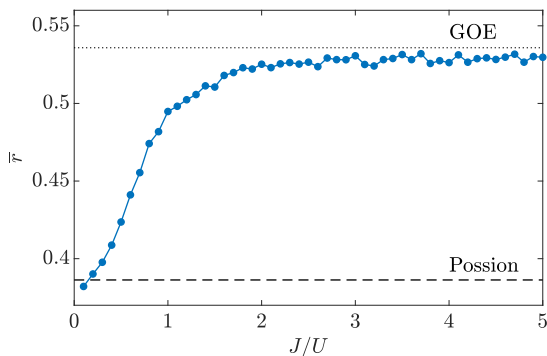


FIG. 6. The mean value \bar{r} for varying values of J/U .

particular charge sector is also investigated in the main

text from a dynamical viewpoint.

To study the statistics of level spacing, we calculate the ratio of consecutive level spacings and then compare the resulting distribution with the established outcomes of the Poisson and Wigner-Dyson distributions. Assuming that E_n is the n -th energy level of the ordered energy spectrum in the charge sector $\hat{Q}^{\text{OBC}} = 2^{L-1}$, we compute the quantity

$$r_n = \frac{\min(s_{n-1}, s_n)}{\max(s_{n-1}, s_n)}, \quad (11)$$

where $s_n = E_{n+1} - E_n$. Then the distributions of r_n for different choices of J/U are compared with the results of the random matrix theory [48, 49]. As shown in Fig. 5, as the parameter J/U increases, the distribution of r_n transitions from a Poisson distribution to a Wigner-Dyson distribution of the Gaussian orthogonal ensemble

(GOE). This crossover is also manifested in the mean value $\bar{r} = \langle r_n \rangle$, which undergoes an increase from the Poisson value 0.386 to the GOE value 0.536 [Fig. 6]. These results indicate that the model is quantum chaotic in the breakdown condensate phase.

Numerical calculation of the phase diagram

In the main text, we employ the spatially dependent Gutzwiller wavefunction to variationally find the mean-field ground state. As introduced in the main text, the wavefunction ansatz is given by

$$|\Phi\rangle = \prod_{m=1}^L \left(\sum_{n=0}^{N_{\max}} C_{m,n} \frac{(\hat{a}_m^\dagger)^n}{\sqrt{n!}} \right) |0\rangle. \quad (12)$$

Under this assumption, the local complex coherent field $\phi_{a,m} = \langle \hat{a}_m \rangle$ can be expressed as

$$\phi_{a,m} = \frac{\langle \Phi | \hat{a}_m | \Phi \rangle}{\langle \Phi | \Phi \rangle} = \frac{\sum_{n=0}^{N_{\max}-1} C_{m,n}^* C_{m,n+1} \sqrt{n+1}}{\sum_{n=0}^{N_{\max}} |C_{m,n}|^2}. \quad (13)$$

Similarly, the local pairing function $\phi_{aa,m} = \langle \hat{a}_m \hat{a}_m \rangle$ is given by

$$\begin{aligned} \phi_{aa,m} &= \frac{\langle \Phi | \hat{a}_m \hat{a}_m | \Phi \rangle}{\langle \Phi | \Phi \rangle} \\ &= \frac{\sum_{n=0}^{N_{\max}-2} C_{m,n}^* C_{m,n+2} \sqrt{(n+1)(n+2)}}{\sum_{n=0}^{N_{\max}} |C_{m,n}|^2}. \end{aligned} \quad (14)$$

The expression is similar for the density operator:

$$\langle \hat{n}_m \rangle = \frac{\langle \Phi | \hat{a}_m^\dagger \hat{a}_m | \Phi \rangle}{\langle \Phi | \Phi \rangle} = \frac{\sum_{n=0}^{N_{\max}} n |C_{m,n}|^2}{\sum_{n=0}^{N_{\max}} |C_{m,n}|^2}. \quad (15)$$

As a result, the energy density of this wavefunction is

$$\begin{aligned} \mathcal{E}_\Phi(\{C_{m,n}\}) &= \frac{\langle \Phi | H | \Phi \rangle}{L \langle \Phi | \Phi \rangle} \\ &= \frac{1}{L} \sum_{m=1}^L \frac{\sum_{n=0}^{N_{\max}} [-\mu n + Un(n-1)/2] |C_{m,n}|^2}{\sum_{n=0}^{N_{\max}} |C_{m,n}|^2} \\ &\quad - \frac{\gamma}{L} \sum_{m=1}^{L-1} (\phi_{a,m} \phi_{a,m+1}^* + \phi_{a,m}^* \phi_{a,m+1}) \\ &\quad - \frac{J}{L} \sum_{m=1}^{L-1} (\phi_{a,m} \phi_{aa,m+1}^* + \phi_{a,m}^* \phi_{aa,m+1}). \end{aligned} \quad (16)$$

Numerically minimizing this energy function with respect to the complex variational parameters $C_{m,n}$ provides the ground-state phase diagram of the $\gamma = 0$ bosonic quantum breakdown Hubbard model, which is shown in Fig.1(a) of the main text.

As for Fig. 2(a) in the main text, the optimization of the energy function involves three different assumptions of the variational parameter space: real positive, real, and complex variational parameters. The final results are then selected from these three outcomes by comparing the resulting ground-state energies. This comparison approach effectively mitigates the potential convergence to local minima above the global minimum of the energy function. In particular, when $J > 0$ and $\gamma > 0$, the results restricted in the space of real positive variational parameters produce the minimum energy of the breakdown condensate phase. This observation indicates that in the breakdown condensate phase, $\phi_m > 0$ is real positive.